

MONITORING CRACK PROPAGATION AT THE ROCK-CONCRETE INTERFACE UNDER DIFFERENT STRAIN RATES USING DIGITAL IMAGE CORRELATION TECHNOLOGY

YAO JIEXIANG¹, DONG WEI^{1*} AND YUAN WENYAN¹

¹State Key Laboratory of Coastal and Offshore Engineering, Dalian University of Technology

Linggong Road 2, Dalian, 116024, China.

e-mail: yaojiexiang@mail.dlut.edu.cn

e-mail: dongwei@dlut.edu.cn (*Corresponding author)

e-mail: yuanwenyan@dlut.edu.cn

Key words: Fracture, Rock-concrete interface, Crack propagation, Rate-dependent

Abstract: In traditional linear elastic fracture mechanics, it is assumed that the stress at the crack tip is infinite. However, in real engineering materials, the ultimate tensile stress is finite, which leads to the formation of a nonlinear micro-cracking zone at the crack tip under applied load. In the context of concrete fracture mechanics, this region is known as the fracture process zone, which plays a crucial role in controlling crack propagation. This study employs Digital Image Correlation technology to measure the full-field displacement and strain throughout the loading process under both natural and saturated humidity conditions. By comparing the load-crack mouth opening displacement obtained from Digital Image Correlation with results from clip-on extensometers, the accuracy of Digital Image Correlation in capturing crack opening displacement at different strain rates is validated. The results indicate that the fracture process zone size and crack opening displacement evolve continuously as loading progresses, with the fracture process zone length and crack opening displacement increasing gradually. Additionally, a more pronounced linear distribution is observed at higher loads. The fracture process zone initially expands with increasing load but begins to shrink as the load diminishes. Furthermore, higher strain rates lead to a shorter fracture process zone length and correspondingly higher loads, while under saturated humidity conditions, the fracture process zone forms earlier than under natural humidity.

1 INTRODUCTION

Traditional linear elastic fracture mechanics assumes infinite stress at the crack tip. However, for any practical engineering material, the maximum tensile stress it can withstand is finite. Therefore, for any cracked material in practical applications, the applied load will create a nonlinear microcrack zone at the crack tip. In metallic materials, this zone is referred to as the plastic deformation zone. In concrete fracture mechanics, it is known as the fracture process zone (FPZ), which is an inherent fracture characteristic of concrete. The mechanism behind its formation is highly

complex. Researches[8] conducted detailed research in this area and indicated that among many mechanisms, the interlocking and bridging effects of coarse and fine aggregates in concrete play a controlling role.

Due to the presence of the fracture process zone, concrete cracks exhibit a stable propagation phase before instability. During this phase, fracture parameters determined using linear elastic fracture mechanics exhibit significant size effects. Considering the influence of the fracture process zone is essential for analyzing crack propagation in concrete materials and for accurately assessing

the safety of structures. Moreover, one critical application of fracture mechanics in concrete structures is to trace crack propagation and predict its risk level, thereby enabling effective reinforcement measures to extend the structure's service life. Thus, studying the concrete fracture process, especially the material's fracture properties at any moment during the stable propagation phase, holds great significance for both research and engineering applications. However, because the organizational structure of concrete is a multi-scale and multi-level system, monitoring the development of the fracture process zone is a challenging task. The previously mentioned clip-on extensometer method effectively monitors the length of the fracture process zone but cannot capture the profile or propagation path of the zone. In this chapter, the author employs Digital Image Correlation (DIC) technology to measure the fracture process zone at the rock-concrete interface.

Hobrough[3] first attempted to extract positional information from image matching using digital image correlation (DIC) in 1960. In the context of material systems, the earliest application of this method was by Peter and Ranson[4] who in 1982 compared small regions (referred to as subsets) of digital images from before and after deformation. By analyzing these comparisons, they determined the post-deformation positions of each subset. During this process, basic concepts of continuum mechanics were employed to control the deformation of the small regions as part of the "matching process." Using this approach, Sutton et al.[6] developed numerical algorithms and conducted preliminary experiments with optically recorded images. This method, now known as two-dimensional digital image correlation (2D-DIC), was further advanced to enhance the speed of analysis. Sutton et al.[5] demonstrated the use of gradient search methods to achieve subset matching with sub-pixel precision across entire images, enabling dense, full-field two-dimensional displacement measurements. Over the following decade, these procedures were validated, modified, and improved[7].

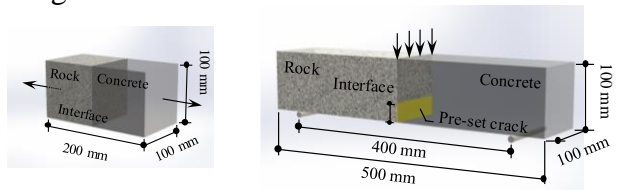
In the late 1980s, early work by Bruck et

al.[1] demonstrated the use of 2D-DIC for stress intensity factor estimation. Sutton et al. used measurements of local crack-tip plastic zones to estimate regions affected by "three-dimensional effects." Dawicke and Sutton[2] employed 2D-DIC to measure crack opening displacements. In recent years, due to its simplicity of operation, algorithmic maturity, and high precision, DIC has been increasingly used by researchers in fracture studies to investigate crack propagation processes.

The study determines the length, width, and profile of the fracture process zone in rock-concrete composite specimens under different humidity conditions (natural and saturated). The crack propagation morphology at various stages is visually presented in the form of three-dimensional images.

2 PREPARATION OF SPECIMENS

Two types of composite concrete-rock specimens were prepared: prisms for assessing interface tensile strength through direct tensile (DT) tests, and beams for evaluating interface fracture properties via three-point bending (TPB) tests. The diagrams of the DT test and the TPB fracture test are shown in Figure 1(a) and (b), respectively. The prism specimens had dimensions of 200 mm × 100 mm × 100 mm (length × width × height), while the beam specimens had dimensions of 500 mm × 100 mm × 100 mm. The supporting span for the TPB fracture test was set at 400 mm, equivalent to four times the specimen height. The pre-set crack length was 30 mm, corresponding to 0.3 times the specimen height.



(a) DT test

(b) TPB test

Figure 1 Diagrams of the DT test and the TPB test

In this study, the concrete mixture was composed with a weight ratio of 1:0.62:1.8:4.2 for cement, water, sand, and aggregate,

respectively, with a maximum aggregate size of 10 mm. The granite rock, obtained from Liaoning Province, China, underwent a surface grooving process using a cutting machine to enhance its roughness. As shown in Fig. 2(a), groove lines were etched with a 3.0 mm depth and 2.0mm width, inclined at a 45° angle to the side edges. These groove lines divided the specimen's cross-section into four equal parts. To initiate a pre-set crack, one side of the rock surface was affixed with two layers of PVC sheets measuring 100 mm × 30 mm, as shown in Fig. 2(b). The rock blocks were placed inside the steel molds before concrete casting. The remaining space was filled with concrete mixtures, and the specimens were initially cured in sealed steel molds for two days, followed by 90 days in a standard curing room. The basic mechanical properties at the ages of 28 and 90 days are listed in Table 1, in which E , ν , f_c , and f_{st} denoted elastic modulus, Poisson's ratio, uniaxial compressive strength, and splitting tensile strength, respectively.

Table 1 Basic mechanical properties of concrete and rock

Materials	E (GPa)	ν	f_c (MPa)	f_{st} (MPa)
Concrete (28 days)	26.00	0.238	38.73	3.42
Concrete (90 days)	31.81	0.238	46.66	4.23
Rock	43.00	0.170	142.72	8.21

3 EXPERIMENTAL RESULTS AND DISCUSSION

Under natural humidity conditions, four DIC specimens were prepared, with one beam corresponding to each strain rate ($10^{-5}/s$, $10^{-4}/s$, $10^{-3}/s$, $10^{-2}/s$). The key difference lies in the use of the Digital Image Correlation (DIC) method instead of clip-on extensometers to monitor crack propagation, aiming to directly capture the evolution of the fracture process zone.

Table 1 presents the basic mechanical and fracture parameters of the specimens under the four strain rates, while Figure 2 shows the P - $CMOD$ curves for the specimens under these strain rates.

Table 1 Three-point bending test results under natural humidity

NO.	P_{ini} (kN)	P_{max} (kN)	G_f (N/m)	l_{max} (mm)
DIC-5-N	0.960	1.149	22.627	68.907
DIC-4-N	1.484	1.963	28.519	66.125
DIC-3-N	2.032	2.334	31.945	64.840
DIC-2-N	1.903	2.423	38.849	62.052

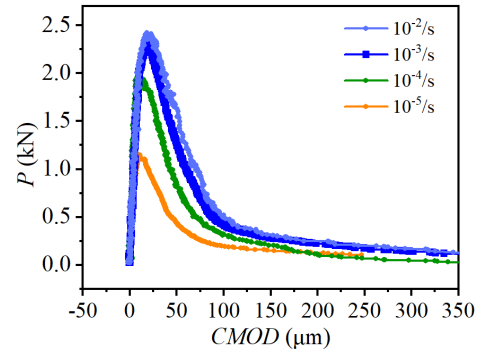


Figure 2 P - $CMOD$ comparison curve under natural humidity

This section analyzes the crack propagation process at the rock-concrete interface under different strain rates from three perspectives: (1) illustrating crack morphology using three-dimensional crack opening images at various load levels; (2) presenting crack propagation paths through strain maps of the fracture process zone under different load levels; and (3) analyzing the variation patterns of crack opening displacement along the ligament direction using crack opening displacement distribution maps at different load levels.

Figure 3 provides a three-dimensional representation of the crack propagation morphology of Specimen Group A under a strain rate of $10^{-5}/s$. In this figure, the vertical axis represents the displacement of pixel points along the x , while the x -axis and y -axis correspond to the coordinates of pixel points in the x -direction and the ligament direction (y -direction), respectively. The origin of the x -coordinate is set at the initial crack tip.

Notably, the z-axis values are positive across all load levels due to an overall leftward movement of the specimen during the experiment. The magnitude of this movement significantly exceeds the crack opening displacement, resulting in positive z-axis values. If no overall displacement occurred, the z-axis values would include both positive and negative values. As shown in Figure 4, the crack opening displacement increases significantly over time, accompanied by an extension of the crack propagation length. At the load level of 23% post-peak, a complete fracture process zone is observed in the specimen, indicating that macroscopic cracks will form at the initial crack tip in the subsequent moment.

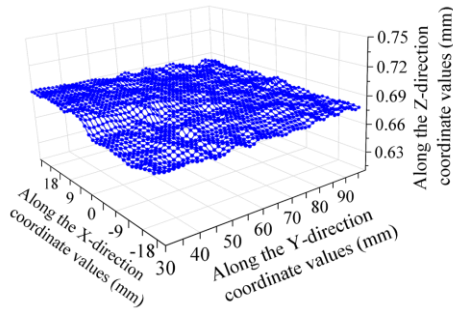


Figure 3 Three-dimensional crack opening diagram at different loading stages at $10^{-5}/s$

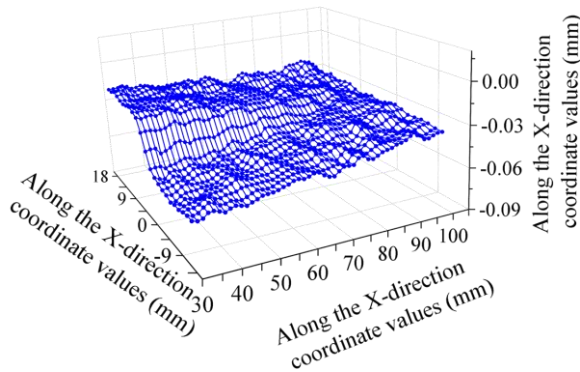


Figure 4 Three-dimensional crack opening diagram at different loading stages at $10^{-4}/s$

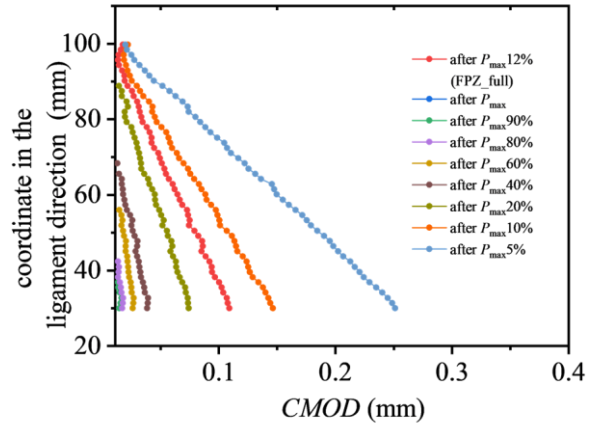


Figure 5 Distribution of crack opening displacement along ligament direction at $10^{-3}s$

Figure 5 illustrates the distribution of crack opening displacements along the ligament under a strain rate of $10^{-4}/s$ at nine representative load levels: the initiation load, peak load, 90% of the peak load, 80% of the peak load, 60% of the peak load, 40% of the peak load, 20% of the peak load, 10% of the peak load, and 12% of the peak load. From the figure, it can be observed that when the load reaches the peak load, the crack tip propagates 8 mm forward from the initial crack tip, reaching a position 38 mm away from the specimen's bottom. At this point, the crack opening displacement at the initial crack tip (i.e., at a vertical coordinate of 30 mm) remains very small. When the load decreases to 80% of the peak load, the crack opening displacement at the initial crack tip increases and continues to propagate forward to a position 42 mm away from the specimen's bottom. At a load level of 12% of the peak load, the crack opening displacement at the pre-crack tip is 0.15 mm, approximately equal to w_0 , indicating that the crack has fully developed in both length and width. At this stage, the crack length represents the complete fracture process zone length, l_{max} , which is 66.125 mm, corresponding to a ratio of 0.944 relative to the ligament length.

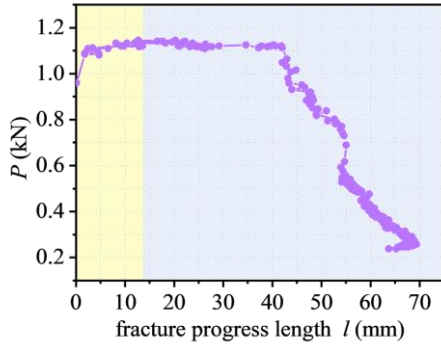


Figure 6 Relationship between FPZ length and load under natural humidity at $10^{-5}/s$

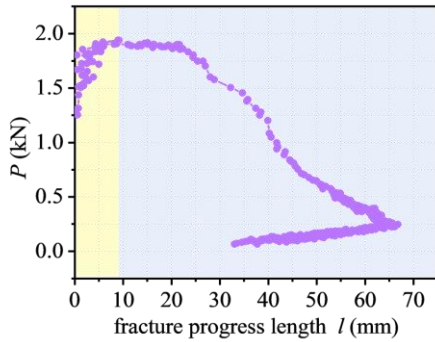


Figure 7 Relationship between FPZ length and load under natural humidity at $10^{-4}/s$

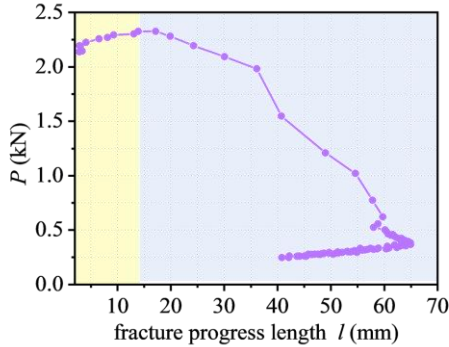


Figure 8 Relationship between FPZ length and load under natural humidity at $10^{-3}/s$

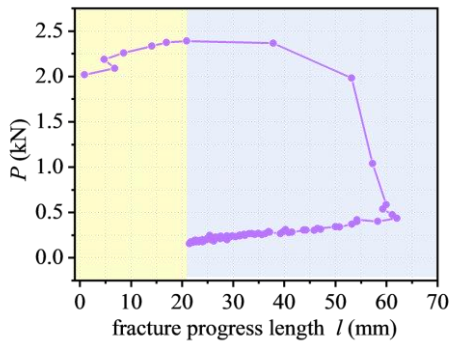


Figure 9 Relationship between FPZ length and load under natural humidity at $10^{-2}/s$

Figure 6 shows the curve of fracture

process zone length versus load under a strain rate of $10^{-5}/s$. From the figure, it can be observed that the initiation load of specimen DIC-5-N is 0.96 kN, and the peak load is 1.149 kN. From crack initiation to the peak load, the crack undergoes a stable propagation stage. After the peak load, as the load decreases, the fracture process zone length increases rapidly. When the load decreases to 0.254 kN, the complete fracture process zone is formed. The analysis process for Figure 7 - Figure 9 is similar. The load values corresponding to the formation of the fracture process zone are 0.331 kN, 0.383 kN, and 0.435 kN, respectively. Comparing the load-fracture process zone curves under the four strain rates, it can be found that as the strain rate increases, the length of the complete fracture process zone decreases, and the corresponding load gradually increases, indicating that the fracture process zone forms earlier.

3 CONCLUSION

This study investigates the crack propagation process under varying strain rates using Digital Image Correlation (DIC) technology. The conclusions drawn are as follows: during crack propagation, the length of the fracture process zone (FPZ) increases with the load. Once the complete FPZ length is reached, the FPZ length decreases as the load reduces. Under natural humidity and saturated humidity conditions, the complete FPZ length decreases with increasing strain rates, while the corresponding load gradually increases.

REFERENCES

- [1] Bruck, H.A. Mcneill, S.R. Sutton, M.A. and Peters, W.H. 1989. Digital image correlation using Newton-Raphson method of partial differential correction. *Experimental Mechanics* **29** (3): 261-267.
- [2] Dawicke, D.S. and Sutton, M.A. 1994. CTOA and crack-tunneling measurements in thin sheet 2024-T3 aluminum alloy. *Experimental Mechanics* **34** (4): 357-368.

- [3] Hobrough G L. 1960. Automatic stereo. *International Archives of Photogrammetry* **4** (13): 1-15.
- [4] Peters, W.H. and Ranson, W.F. 1982. Digital Imaging Techniques In Experimental Stress Analysis. *Optical Engineering* **21**: 427.
- [5] Sutton, M. Mingqi, C. Peters, W. Chao, Y. and McNeill, S. 1986. Application of an optimized digital correlation method to planar deformation analysis. *Image and Vision Computing* **4** (3): 143-150.
- [6] Sutton, M. Wolters, W. Peters, W. Ranson, W. and McNeill, S. 1983. Determination of displacements using an improved digital correlation method. *Image and Vision Computing* **1** (3): 133-139.
- [7] Sutton, M.A. Turner, J.L. Chao, Y.J. Bruck, H.A. and Chae, T.L. 1992. Experimental investigations of three-dimensional effects near a crack tip using computer vision. *Int J Fract* **53** (3): 201-228.
- [8] Xu, S. and Reinhardt, H.W. 1999. Determination of double-Determination of double-K criterion for crack propagation in quasi-brittle fracture Part I: experimental investigation of crack propagation. *International Journal of Fracture* **98** (2): 111-149.